

## The Scattering Mechanisms and Electronic Properties of SiC Semiconductor

M. Khooshebast and H. Arabshahi

Department of Physics, Payame Noor University, Tehran, Iran

### Abstract

We have studied the band structure properties of SiC in wurtzite crystal structures. In our calculations we have adopted a pseudopotential approach based on the Density Functional Theory (DFT). We have calculated the band structure and density of state (DOS). The result shows that the electronic band structure and density of state data for SiC in wurtzite crystal structures are comparable with their experimental calculations. In the second part we have calculated the effective mass of electron in three valley model. And finally in the third part of this survey we have studied piezoelectric, deformation potential and optical phonon scattering mechanisms.

**Key words:** Pseudopotential; Density Functional Theory; Effective Mass; Electron Scattering.

### Band Structure Calculation

First principles or ab-initio approaches provide a method for modeling systems based solely on their atomic coordinates and the Z numbers of the different atoms. These techniques rely on the fact that there should be one unique charge density or distribution which describes the ground state of a system [1]. This reduces the problem of solving for the electronic structure of a system from a 3N dimensional problem to one that only depends on the charge density. A number of approaches have been developed to properly reduce a system to the minimum energy electronic configuration and abinit includes several of these. First principles codes such as abinit have proved useful to topics ranging from the composition of the planetary core to the electrical properties of single molecule. Abinit can calculate the forces on atoms in a structure and use this information to relax the system. This has provided critical understanding in how surfaces reconstruct, how adsorbates interact with surface sites, and how magnetic impurities affect neighbor lattice sites. Typically calculations can consider 30-40 atoms comfortably. Larger systems can be done, but for fairly large systems (greater than 150 atoms), parallel calculations are essential [2-6]. In addition to minimizing the total energy of a structure, abinit can also calculate band structures, density of states, magnetic properties, and phonon dispersion curves. We made a  $6 \times 6 \times 6$  super cell of the unit cell which contain 12 atoms and then substituted some of the Si

atoms by C atoms in wurtzite crystal structure. There are two important parameters which should be optimized correctly for saving time and also to have an acceptable precision in calculations. These parameters are cutoff-energy and kgrid-cutoff where their optimized values were chosen. SiC can crystallize in zincblende, wurtzite and rhombohedral structures, which have slightly different material properties and substantially different band structures [3]. However, the wurtzite phase of SiC is the more stable bulk form of the material and the common form for epitaxial layers. The wurtzite crystal structure of SiC is shown in figure 1. It can be regarded as an interpenetration of two hexagonally close packed (HCP) sublattices with a relative displacement along the c-axis by  $uc$  where  $u$  is the so called internal parameter and  $c$  is the lattice constant for the c-axis. The distance between in-plane atomic neighbors is denoted by  $a$ . For an ideal wurtzite structure  $c/a = (8/3)^{1/2} = 1.633$  and  $u = 3/8 = 0.375$  and the atoms have the regular tetrahedral coordination of nearest neighbors that occurs for the zincblende structure [4]. The difference between the two structures is in the next nearest neighbor arrangement. The first Brillouin zone of wurtzite SiC which is a hexagonal prism of volume is shown in figure 1 as well together with the locations of the high-symmetry points  $\Gamma$ , K, M and U [5,6].

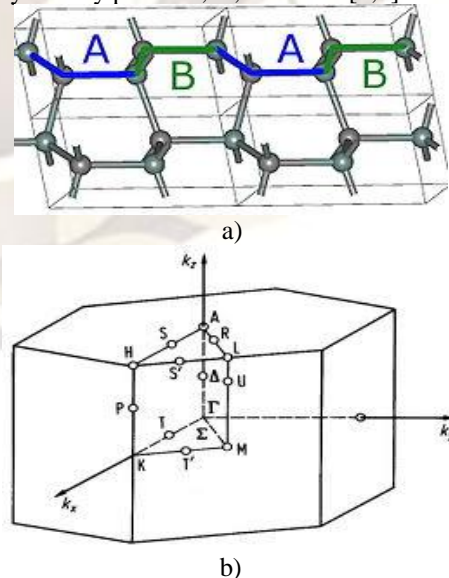


figure1. a) The crystal structure of wurtzite SiC and b) the first brillouin zone of a wurtzite.

The calculated band structure of 2H-SiC in wurtzite crystal structure has been shown in figure 2. The obtained band gap for 2H-siC is about 2.2 eV. For SiC the top of the valance band is at the K point, and it has an indirect band gap. The real band gap in this crystal will be somewhat larger on the order of about 1 eV.

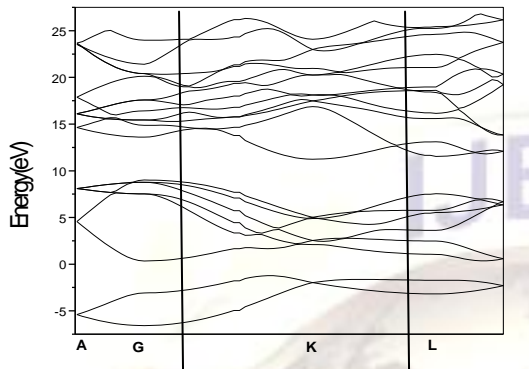


figure2. The band structure of 2H-SiC

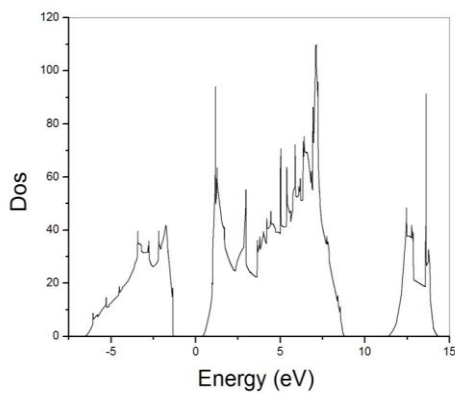


figure 3. The calculated total density of states in 2H-SiC.

Table 1 summarizes the values of lowest indirect forbidden gaps ( $E_g$ ) for 2H-SiC from our model, as well as theoretical results from LDA, GW and experimental results. The discrepancies of the energy gap between the GW and experiment are around 0.01 eV. Our result is in very good agreement with the experimental data [7] and pseudopotential *ab initio* results including the GW approximation [8] as listed in Table 1.

Table 1: Values of indirect gap (in eV) of SiC.

valley	$\Gamma$	K	U	
Effective mass	$0.08 m_0$	$0.16 m_0$	$0.8 m_0$	
Method	This Work	LDA	GW	Experiment
Band Gap	2.23	2.10	3.31	3.30

### 1. Effective Mass

In this section we shall present a general model for the band structure which enables us to interpret the macroscopic properties of the semiconductors of interest in devices.

The model consists of one conduction band, with three sets of minima in the region around the minima of the conduction band, the function  $E(\mathbf{k})$  can be approximated by a quadratic function of  $\mathbf{k}$  :

$$E(\mathbf{k}) = \sum_{i,j} \frac{\hbar^2}{2} \left(\frac{1}{m}\right)_{ij} k_i k_j \quad (1)$$

$$\text{Where } \left(\frac{1}{m}\right)_{ij} = \frac{1}{\hbar^2} \left(\frac{\partial^2 E}{\partial k_i \partial k_j}\right) \quad (2)$$

Is the inverse effective mass tensor, and  $\mathbf{k}$  is measured from the centers of the valleys. In the model considered here  $E(\mathbf{k})$  is assumed in following from [9]:

$$E(\mathbf{k}) = \frac{\hbar^2}{2} \left[ \frac{k_l^2}{m_l} + \frac{k_t^2}{m_t} \right] \quad (3)$$

Equation (3) represents a band with ellipsoidal equi-energetic surfaces, with tensor effective mass. The ellipsoids have rotational symmetry around the crystallographic directions which contain the centers of the valleys. Here,  $k_l$  and  $k_t$  are the longitudinal and transverse components of  $\mathbf{k}$  with respect to these directions;  $\frac{1}{m_l}$  and  $\frac{1}{m_t}$  are the longitudinal and transverse

components, respectively, of the inverse effective mass tensor. For values of  $\mathbf{k}$  from the minima of conduction band, the energy deviates from the simple quadratic expression, and nonparabolicity occurs. For the conduction band, a simple analytical way of introducing nonparabolicity is to consider an energy-wave vector relation of type [10]

$$E(1 + \alpha E) = \gamma(k) \quad (4)$$

Where  $\gamma(k)$  is given by the right-hand side of Eqs. (3).  $\alpha$  is a nonparabolicity parameter [11-13].

By using equations (3) and (4) the effective mass in conduction band for 2H-SiC has been calculated in  $\Gamma$ , K and U valleys and the result is shown in table (1)

Table1: Calculated effective mass for 2H-SiC in  $\Gamma$ , K and U valley.

### 3. Scattering Mechanisms

As usual in semi-classical transport, the dynamics of electron interactions is assumed to be

independent of the applied field, and the collisions are assumed to occur instantaneously.

All scattering calculations presented here will be carried out with a first order perturbative approach, consequently only two-body interactions will be analyzed.

The electronic transitions of interest for charge transport in semiconductors can be classified as intra valley when the initial and final states lie in the same valley, or inter valley when they lie in different valleys.

The most important sources of scattering that determine these transitions in the bulk of homogeneous crystals are phonons and impurities.

The interaction of phonons with charge carriers is due to the deformation of the otherwise perfect crystal produced by phonons through the deformation potential mechanism or through the electrostatic forces produced by the polarization waves that accompany the phonons. It is useful to present a physical discussion of the main features of each scattering process with particular attention to their influence on carrier transport.

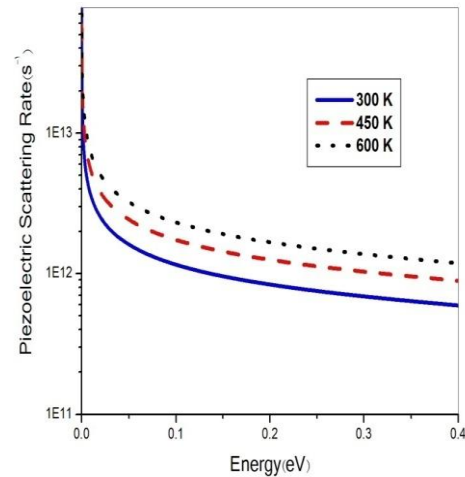
#### a) Acoustic Scattering With Piezoelectric and Interaction Deformation Potential

The maximum energy transfer for an electronic interaction with acoustic phonons is, in general, much smaller than the electron energy, and thus very often acoustic scattering is treated as an elastic process. The electrostatic nature of this mechanism leads to a scattering efficiency that decreases at increasing carrier energy; its importance is restricted to low temperature and low field situations, especially in high-purity materials. In dealing with hot-electron problems, where its influence is negligible, the piezoelectric scattering should always be considered together with the scattering due to deformation-potential interaction.

As is shown in figures 4 and 5 you can see the piezoelectric and deformation-potential scattering rates as a function of electron energy for acoustic phonons for SiC semiconductor in different temperatures.

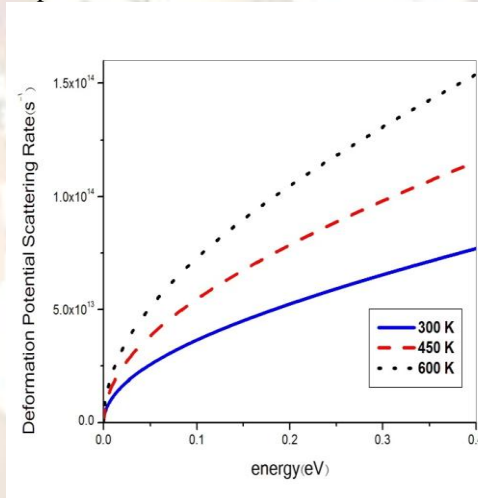
As is shown in figure 4, by increasing the temperature the scattering rate increases and for high energy electrons, the scattering rate decreases.

As is shown in figure 5, by increasing the temperature the scattering rate increases, and by increasing the electron energy, the scattering rate increases from 0 to  $7 \times 10^{13}$  in room temperature.



Fi

Figure 4. Energy dependence of the piezoelectric scattering rate in gamma valley of SiC at different temperatures.



Fi

Figure 5. Energy dependence of the deformation-potential scattering rate in gamma valley of SiC at different temperatures.

#### b) Optical-Phonon Scattering with Deformation-Potential Interaction.

Usually the equivalent temperature of the optical phonons is assumed to be constant since the dispersion relation of such kind of phonons is quite flat for the  $q$  values involved in electronic intra valley transitions. As we shall see, this kind of scattering is isotropic.

#### c) Optical-Phonon Scattering With Polar Interaction

The electrostatic nature of interaction is such that forward scattering is favored, so that this mechanism is strongly anisotropic. The treatment of this scattering is simplified by the constancy of the phonon energy in the transition. At high electron energies the total scattering rate for polar optical scattering decreases with increasing energy.

Optical phonon scattering rate in phonon emission and absorption as a function of energy in  $\Gamma$  valley for 2H-SiC are shown in figures 6 and 7 for different temperatures.

As you can see in figure 6 electron can absorb phonon in a high rate specially in low energies. By increasing the temperature, the scattering rate increases too. By increasing the electron energy from 0 to 0.4 eV the scattering rate varies from  $5.2 \times 10^{12}$  to  $3 \times 10^{12}$ .

As you can see in figure 7 the probability of emission is obviously zero when  $E < \hbar\omega_{op}$ , since the carrier does not have enough energy to emit the phonon. It is also known that by increasing to the temperature, the scattering rate increases.

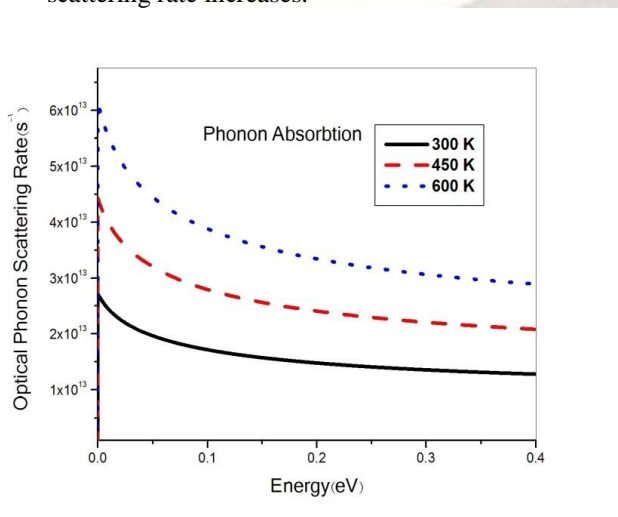


Figure6. Energy dependence of the optical phonons scattering rate in gamma valley of SiC at different temperatures for phonon absorption.

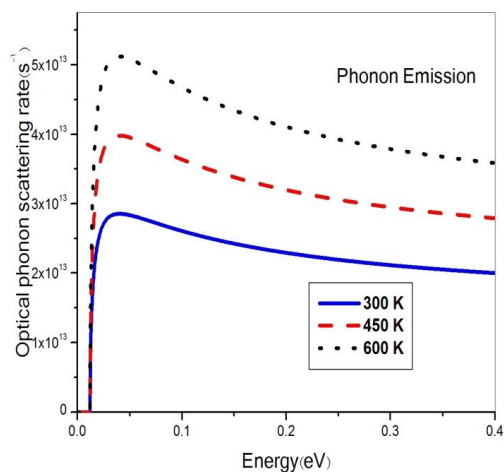


Figure7. Energy dependence of the optical phonon scattering rate in the gamma valley of 2 SiC at different temperatures for phonon emission.

## References

- [1] X. Gonze, J.-M. Beuken, R. Caracas, F. Detraux, M. Fuchs, G.-M. Rignanese, L. Sindic, M. Verstraete, G. Zerah, F. Jollet, M. Torrent, A. Roy, M. Mikami, Ph. Ghosez, J.-Y. Raty, D. C. Allan, *Comput. Mater. Sci.* 25, 478 (2002).
- [2] A. M. Rappe, K. M. Rabe, E. Kaxiras, J. D. Joannopoulos, *Phys. Rev. B* 41, 1227 (1990)
- [3] Numerical Data and Functional Relationships in Science and Technology, edited by O. Madelung, Landolt-Bornstein, New Series, Group 3, vol. 17, Pt. a (Springer-Verlag, New York), (1982)
- [4] A. R. Verma and P. Krishna, *Polymorphism and Polytypism in Crystals* (Wiley, New York, 1966), Chap. 5.
- [5] Properties of Advanced semiconductor Materials GaN, AlN, InN, BN, SiC, SiGe, M. E. Levinshtein, S. L. Rumyantsev, and M. S. Shur, Eds. New York: Wiley, 2001, pp. 31-47.
- [6] M. Ruff, H. Mitlehner, and R. Helbig, "SiC devices: physics and numerical simulation", *IEEE Trans. Electron Dev.*, vol. 41, pp. 1040-1053, 1994
- [7] K. H. Hellwege (ed.), Landolt-Börnstein, Numerical and Functional Relationships in Science and Technology (Springer-Verlag, Berlin, 1982).
- [8] B. Wenzien, P. Käckell, F. Bechstedt, and G. Cappellini, *Phys. Rev. B* 52, 10897 (1995).
- [9] Smith, R. A.: *Semiconductors*. Cambridge: Cambridge University Press 1964.
- [10] Conwell, E. M., Vassel, M.O.: *Phys. Rev.* 166,797(1968).
- [11] Fawcett, W., Boardman, D. A., Swain, S.: *J. Phys.* 55, 645 (1983).
- [12] Paige, E. G. S.: *The Electrical Conductivity of Germanium* (Gibson, A. F., Burgess, R. E., eds.). London: Heywood. 1964.